

WHERE IS THE MOBILITY EDGE IN AMORPHOUS SEMICONDUCTORS?

Keiji Tanaka, Shin-ichi Nakayama*

Department of Applied Physics, Faculty of Engineering, Hokkaido University,
Sapporo 060-8628, Japan

Photoconduction measurement of chalcogenide glasses such as As_2Se_3 at low temperatures show that the fundamental photoconductive edge is located at nearly the same photon energy with the absorption edge in the corresponding crystals. This coincidence implies that the mobility edges of the conduction and the valence band in amorphous semiconductors exist at the same energies with the band edges in the crystalline counterparts. Other spectral data are also reviewed from this viewpoint.

(Received February 9, 2000; accepted February 16, 2000)

Keywords: Mobility gap, Amorphous semiconductor, Chalcogenide glass, Photoconduction

1. Introduction

Much work has been done for the understanding of electronic structures in amorphous semiconductors [1-3], while some fundamental problems still remain unresolved. Among these, one of the most important may be the identification of several bandgap energies employed to characterize amorphous semiconductors. For instance, the interpretation of the Tauc optical gap has not yet been established. The mobility-gap concept has been employed frequently, while we do not know the gap energy. Relations between these gaps and the bandgap in the corresponding crystal are still vague. In the present work, therefore, we study the bandgap energy in amorphous semiconductors, specifically, focusing upon the problem where the mobility edge exists in real materials.

As pointed out by Mott, the mobility gap may be estimated from spectral photoconductive measurements at low temperatures [1]. However, to the authors' knowledge, no reliable spectral measurements have been reported, probably because photocurrents become substantially smaller at lower temperatures [1,3]. In addition, to evaluate the mobility gap with a reasonable accuracy, photoconductive spectra should be determined over wide absorption regions.

Accordingly, we will try to evaluate the mobility gap using the constant-photocurrent method (CPM) in conjunction with special electrodes. In addition, previous spectral data are reviewed, and several bandgap energies are compared with the crystalline bandgap. Simple chalcogenide glasses are examined mainly, since a-Si(Ge) appear to be much defective and for hydrogenated amorphous films no comparable crystalline materials are available. We will see that the photoconductive edge is located at nearly the same photon energy with the bandgap of the corresponding crystals. It seems that the crystalline bandgap determines the mobility gap in amorphous semiconductors.

2. Bandgap energies in amorphous semiconductors

We know, at least, four bandgap energies, which can be experimentally evaluated (see Table 1). An electrical bandgap energy, two optical bandgap energies, and the one derived from dispersion spectra.

*Now, member of Fujitsu Ltd.

Table 1. Some threshold energies in unit of eV evaluated at low temperatures ($\leq 100\text{K}$) and at room temperature (shown with parentheses). E_σ is the electrical activation energy, E_g^T the Tauc gap, E_x the optical ultimate energy (see, the text), E_0 the average gap, E^{FR} the gap evaluated from Faraday rotation, E^{PL} evaluated from photoluminescence, E^{PC} the photoconductive gap, and E_g^{cryst} is the gap in the corresponding crystal. For GeS(Se)2, deposited films are defective and Tauc gaps cannot be evaluated using bulk glasses, and accordingly the listed E_g^T are estimated from Urbach tails. *indicates a preliminary result.

Material	Se	As ₂ S ₃	As ₂ Se ₃	As ₂ Te ₃	GeS ₂	GeSe ₂
$2E_\sigma$	(2.2) [2]	(2.3) [2]	(1.8) [2]	(0.8) [32]	1.4 [2]	1.9 [2]
E_g^T	2.1 [1]	2.5 [1]	1.9 [7]	1.0 [32]	3.2 [27]	(2.2) [2]
E_x	2.4 [7]	(2.7) [6]	2.1 [7]			
$E_0/1.5$	(2.9) [9]	(3.1) [9]				
E^{FR}	(2.1) [10]	3.1 [10]	2.4 [10]			
E^{PL}		2.6 [13]			(3.7)	3.0
E^{PC}	2.7	2.7	2.1	1.0*		2.3 [13]
E_g^{cryst}	1.7-3.0 [23]	2.8 [19]	2.0 [19]	(0.9) [24]	3.8 [25]	2.5 [26]

The electrical bandgap energy is obtained by doubling the activation energy E_σ of dc electrical conductivity [1-3]. The conductivity σ at around room temperature can be fitted as $\sigma \propto \exp(-E_\sigma/k_B T)$, in which E_σ is assumed to give the separation between the Fermi energy and the mobility edge of mobile carriers, which are holes in most chalcogenide glasses. Accordingly, if the Fermi energy were located at the center of the mobility gap, $2E_\sigma$ would give the gap energy.

The next is optical bandgaps. It is known that the optical absorption edge in many amorphous semiconductors can be fitted with three spectral functions [1-3]; from high to low absorption regions, the absorption coefficient α being proportional to $(\hbar\omega - E_g^T)^2/\hbar\omega$ at $\alpha \geq 10^4 \text{ cm}^{-1}$, $\exp(\hbar\omega E_U)$ at $\sim 10^2 \text{ cm}^{-1}$, and $\exp(\hbar\omega E_W)$ at $\sim 10^0 \text{ cm}^{-1}$. Here, E_g^T is the so-called Tauc gap energy, E_U is the Urbach energy, and E_W characterizes the weak-absorption tail. Although the interpretation of these spectral functions still remains ambiguous [1-5], E_g^T has been employed frequently as the optical bandgap energy [1-3].

Recently, some theoretical and experimental studies have demonstrated that an optical bandgap energy E_g in amorphous semiconductors can be expressed as $E_g \approx E_x - \alpha E_U$ [3-7]. Here, E_x is an ultimate energy and α is a constant. Some theoretical studies [4,5] assert that both the Tauc gap and the Urbach energy are influenced from structural disorder, and that E_x represents the bandgap energy in disorder-free materials.

The fourth is the one derived from dispersion spectra. For instance, the single-oscillator model proposed by Wemple and DiDomenico shows that the refractive-index $n(\omega)$ at $\hbar\omega < E_g$ can be written down as $n(\omega)^2 - 1 = E_d E_0 / (E_0^2 - \hbar^2 \omega^2)$, where E_0 and E_d are termed as the average gap and the dispersion energy [8,9]. E_0 is interpreted as a measure of the separation between the centers of the valence and the conduction band, and empirically $E_0/1.5$ is demonstrated to give a rough estimate of a *direct* bandgap energy [8]. The bandgap energy E^{FR} obtained from Faraday rotation measurements appears to have a similar character to that of $E_0/1.5$ [10].

In addition to these empirical energy gaps, the mobility gap has been frequently employed as a theoretical concept after Cohen, Fritzsche, Ovshinsky and Mott [11]. It is assumed that the mobility gap exists between mobility edges (in the conduction and the valence band), which separate localized

from extended states. Carriers being located in the mobility gap are assumed to be completely immobile at 0 K.

However, the concept of the mobility edge seems to be still vague. Little work has been reported for the value of the mobility gap in real materials [11-13], and theoretical studies predicting mobility-edge energies are few. No reliable experimental methods have been established for evaluating the mobility gap. The relationship between the mobility gap and the other empirical gaps is unclear, and accordingly, we are still unconvinced of the mobility-gap concept.

3. Experiments

Samples investigated in the present CPM measurement were a-Se, and four kinds of stoichiometric chalcogenide glasses, As_2S_3 , As_2Se_3 , GeS_2 and GeSe_2 . Se films were prepared by vacuum evaporation. For the binary glasses, polished bulk samples were employed after annealing at the glass-transition temperatures [14]. Electrodes employed were a planar interdigital type (20-pair fingers, 10 μm gap-separation, 1 mm gap-width) made of Au films, and CPM spectra were measured using a conventional cw/dc system. Details are described in [15].

4. Results

Fig. 1 shows a series of CPM spectra for As_2Se_3 at 10-350 K. Also shown in figure are the optical absorption spectra at 10 K (dashed line) [16] and 300 K (solid line) [1]. Although the CPM is a powerful method for evaluating small absorption, absolute absorption coefficients cannot be determined from CPM spectra alone [3]. Accordingly, in the figure we have followed the conventional way for fixing the vertical positions [15]. That is, the spectra are plotted so that these overlap the Urbach tail (at 300 K) or the extrapolated one (at 10K) at $\alpha d \approx 1$, where d is an effective sample thickness [17]. Spectra at other temperatures are positioned taking the temperature dependence of the optical absorption edge [16] into account.

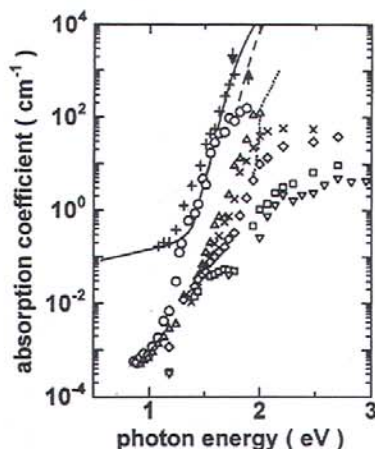


Fig. 1. CPM spectra in As_2Se_3 glass at 10 K (∇), 100 K (\square), 150 K (\diamond), 200 K (\times), 250 K (Δ), 300 K (\circ) and 350 K ($+$). Also shown are optical absorption spectra in the glass at 10 K (dashed line) [16] and 300 K (solid line) [1], for which Tauc gaps are indicated by the arrows, and an absorption spectrum in the corresponding crystal at 10 K (dotted line) [19].

In this figure, the optical absorption spectra show some universal features [1-3]. The spectrum at 300 K [1] exhibits the square-law dependence, the Urbach tail, and the weak-absorption tail. The 10 K spectrum gives only the square law at $\alpha \geq 10^2 \text{ cm}^{-1}$ [16]. From the square-law spectra, we see

that the Tauc gap is 1.8 eV at room temperature [1] and it increases to 109 eV at 10 K [16]. Such spectral and temperature dependences are commonly in many amorphous semiconductors [1-3].

In contrast, the CPM spectra in Fig. 1 shows three marked features. First, photocurrent signals corresponding to the weak-absorption tail are not scarcely detected, specifically at low temperatures. The reason has been discussed previously in connection with band-tail structures [15]. Second, in addition to the spectral shift to higher energies, at low temperatures, the photoconductive Urbach tail does not follow simple exponential curves. It is evident that distinct shoulders appear at $\hbar\omega \approx 1.7$ eV and $\alpha \approx 10^{-1} \text{ cm}^{-1}$ at $T \leq 150$ K, although data points necessarily become fewer at lower temperatures due to smaller photocurrents [18]. Extrapolating the optical Urbach edge at 10 K lower absorption regions, we see that the shoulder forms a non-photoconducting spectral gap, or a photocurrent-suppressed region. This feature is reminiscent of the spectral gap in a-Se at room temperature [1], and the existence has been understood on the basis of geminate recombination models [1,15]. Polaron formation may also contribute to the gap [1,3]. Above the non-photoconducting spectral gap, the CPM spectra manifest steep rises and we can define the *photoconductive spectral edge* E^{PC} there. Third, the CPM spectra show some saturation at higher absorption regions, i.e. $\alpha \geq 10^0 \text{ cm}^{-1}$ at low temperatures or at $\hbar\omega \geq 2.0$ eV at high temperatures. This saturation is probably due to surface effects, transport properties, and/or deviation from a CPM presumption; that is, the CPM can provide linear photocurrent signals only when $\alpha d \leq 1$ [3]. Accordingly, the CPM spectra in the saturated region should be neglected.

Similar CPM spectra have been obtained for other samples [15] and Fig. 2 shows an example for GeS_2 . In comparison with As-chalcogenides, Ge-chalcogenide glasses are difficult to prepare and less photoconductive and accordingly, the data are less accurate.

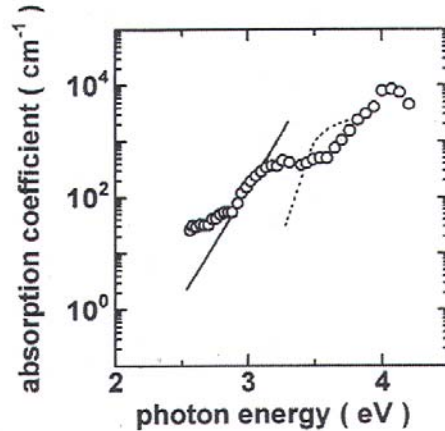


Fig. 2. A CPM spectrum in GeS_2 at room temperature (\circ). Also shown by solid and dotted lines are optical absorption spectra in the glass, obtained in the present study, and in the crystal [25].

Fig. 3 summarizes the temperature dependence of the photoconductive edge E^{PC} by solid lines. Here, the determination of E^{PC} is somewhat arbitrary, since the photoconductive edge is not very sharp. If E^{PC} is evaluated at the threshold energy of the steep photoconduction rise, E^{PC} at low temperatures decreases by 0.1 eV for As_2Se_3 . Therefore, to compare the photoconductive results with optical data, E^{PC} and corresponding optical absorption edges are evaluated at the selected absorption coefficients, which are written in the figure caption.

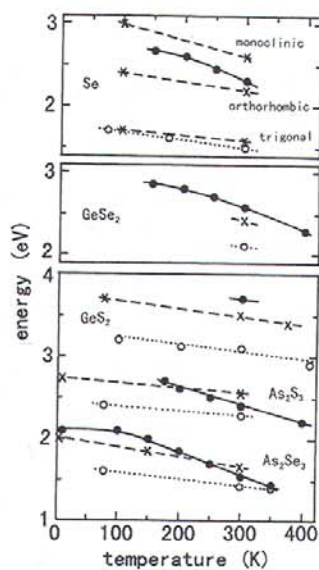


Fig. 3. Temperature dependence of the photoconductive edge (*connected with solid lines) and the optical absorption edge (\circ with dotted lines) [1,2,27] in the glasses denoted, and the band edge (\times with dashed lines) in related crystals [19,20,23,25]. For Se and As_2Se_3 the edge positions are estimated at $\alpha \approx 10^0 \text{ cm}^{-1}$, for As_2S_3 and GeSe_2 at 10^2 cm^{-1} , and for GeS_2 at 10^5 cm^{-1} , which are selected for feasible comparisons. Accuracy in the energy scale is typically $\pm 0.1 \text{ eV}$.

5. Discussion

Fig. 1 also shows by a dotted line the optical absorption edge in the layer-type As_2Se_3 crystal at 10 K [19]. Due to a limited size of the samples, the spectrum is obtained only for the electric field directing in parallel to the layer plane ($E \parallel a$ and c) at $\alpha \geq 5 \text{ cm}^{-1}$. We see that the spectrum has a steep rise at $\hbar\omega = 2.0 \text{ eV}$, which is identified through experimental and theoretical analyses as a direct or indirect bandgap [19-21].

We here note that the crystalline absorption edge and the photoconductive edge at 10 K are located at nearly the same photo energy, $\sim 2.0 \text{ eV}$. Such a correspondence is also seen for GeS_2 in Fig. 2.

The photoconduction edge (at low temperatures) is attributable to photoexcitation and successive transport without thermal activation [22] in extended electronic states. Therefore, the edge is assumed to signify the mobility gap [1]. Then, the fact that the edge is located at nearly the same position with the crystalline absorption edge implies that the crystal bandgap determines the mobility gap. Can we find such correspondences in other materials?

Fig. 3 and Table 1 summarize the photoconductive gap E^{PC} and the crystalline gap E_g^{cryst} [19,20,23-26] in other materials. The figure also shows by dotted lines the positions of the (extrapolated) Urbach tails [1,2,27], which are evaluated at comparable absorption coefficients with those for the CPM spectra. Hence, the difference between the two curves approximates the non-photoconducting spectral gap.

We see in Fig. 3 that the correspondence between the photoconductive edge and the crystalline bandgap is held roughly for all the materials. As_2S_3 manifests a good correspondence, in a similar manner to that in As_2Se_3 . For GeSe_2 , crystalline data are available only at room temperature [26], while these are consistent with the relation $E^{\text{PC}} \approx E_g^{\text{cryst}}$.

Situations for Se are complicated. Because, there exist several kinds of crystals, some of which exhibit non-photoconducting edges in amorphous and crystalline forms, the latter being less accurate in absolute absorption values. Accordingly, only some trends are worth to be mentioned. The upper traces in Fig. 3 show that amorphous film and the ring-type crystals (monoclinic and orthorhombic) possess comparable photoconductive gaps. These are located at substantially higher energies than the photoconductive edge in the chain (trigonal) crystal. This similarity between the amorphous and the ring-type crystals may imply that extended electronic states in a-Se resemble those existing in the ring-type crystals [28].

Taking these correspondences between the glassy photoconductive edge and the crystalline band edge at low temperatures into account, we are tempted to assume that the crystalline band edges are responsible for the mobility edges in the glass. That is, the threshold energies separating extended and localized electronic states in the conduction and valence bands in the glass are assumed to be located at the band edges in the corresponding crystal.

The mobility-edge energy has also been evaluated by Murayama through photoluminescence studies [13]. He has investigated the excitation-energy dependence of time-resolved photoluminescence at 4 K, and found that the luminescence peak energy and the polarization memory change with excitation photon energy, showing a threshold at excitation of 2.6 eV for As_2S_3 and 2.3 eV for GeSe_2 . The photoluminescence is assumed to be caused by recombination of localized electron-hole pairs, and accordingly, carriers being excited to extended states must give some different behaviour [1,3]. Then, he concludes that the threshold energy could signify the mobility gap. He also points out that the mobility gap obtained is very close to the absorption edge in the crystalline counterparts (see, Table 1).

From a theoretical point-of-view, the idea that the mobility edge is located at the crystalline band edge can be accepted straightforwardly [29]. If a crystal is distorted, the edges of the conduction and valence bands will tend to move toward the center of the gap. Such band-edge shifts also occur when a crystal is heated, i.e. when a crystal is dynamically disordered. The reason is that the structural symmetry in a crystal is broken and degenerate electronic states undergo energy splitting. Thus, the bandgap appears to become smaller with the structural disordering, while, to the first order, the center of gravity of the split does not move. Therefore, if the disorder in amorphous semiconductors is characteristically common to this broken symmetry, the band edge of the crystal may determine the mobility edge in the disordered material. Some computer calculations upon Si seem to support this hypothesis [29,30], and similar analyses for chalcogenide glasses will be valuable.

The idea that the mobility edge is located at the band edge in a corresponding crystal can also be supported by the two structural features. The first is the structural similarity between the glass and the corresponding crystal [1-3]. The glassy structure is known to retain short-range structural order resembling the corresponding crystalline structure, while lacking in long-range periodicity, and accordingly, the crystalline band edge may leave some trace upon the mobility edge. The second applies specifically to the chalcogenide glass. That is, the unit cells of stoichiometric chalcogenide crystals such as $\text{As}_2\text{S}(\text{Se}, \text{Te})_3$ and $\text{GeS}(\text{Se})_2$ are large, which makes the Brillouin zones small. Thus, the dispersion curve tends to become flat, as demonstrated by some theoretical calculations [21,31,32]. Structural order being limited within a distance of Δr produces a wavenumber uncertainty of Δk , while since the dispersion curve is rather flat the k uncertainty is less effective. Accordingly, the dispersion curve can be a good approximation for the electronic structure in chalcogenide glasses, and the band edge may govern the mobility edge.

6. Summary

It has been demonstrated for some chalcogenide glasses that the photoconductive spectral gap is located at the same energy position as the band gap in the crystalline counterparts. This correspondence implies that the mobility edges in the glass are located at the band-edge positions in the crystal.

Such an electronic similarity must reflect the structural similarity in amorphous and crystalline semiconductors. A more essential and open question is, therefore, why the structural order can exist in the glass.

Acknowledgement

The present work was partially supported by a Grant-in-Air for Scientific Research from the Ministry of Education, Science, Sport and Culture.

References

- [1] N. F. Mott, E. A. Davis, *Electronic Processes in Non-Crystalline Materials*, Clarendon Press, Oxford, 1979.
- [2] S. R. Elliott, *Materials Science and Technology*, **9**, edited by J. Zarzycki, VCH, Weinheim, Chap. 7, (1991).
- [3] K. Morigaki, *Physics of Amorphous Semiconductors*, Imperial College Press, London, 1999.
- [4] H. Okamoto, K. Hattori, Y. Hamakawa, *J. Non-Cryst. Solids*, **198-200**, 124 (1996).
- [5] S. K. O'Leary, *Appl. Phys. Lett.*, **72**, 1332 (1998).
- [6] K. Tanaka, *Phys. Rev.*, **B36**, 9746 (1987).
- [7] J. Pétursson, J. M. Marshall, A. E. Owen, *Philos. Mag.*, **B63**, 15 (1991).
- [8] S. H. Wemple, Jr. M. DiDominico, *Phys. Rev. Lett.*, **23**, 1156 (1969).
- [9] S. H. Wemple, *J. Chem. Phys.*, **67**, 2151 (1977).
- [10] P. Van den Keybus, B. Vanhuysse, W. Grevendonk, *phys. stat. sol. (b)*, **98**, 551 (1980).
- [11] G. S. Higashi, M. Kastner, *Phys. Rev. Lett.*, **47**, 124 (1981).
- [12] M. A. Bösch, G. S. Higashi, M. Kastner, *Phys. Rev. Lett.*, **48**, 649 (1982).
- [13] K. Murayama, *J. Non-Cryst. Solids*, **59&60**, 983 (1983).
- [14] It is known that deposited GeS(Se)₂ films are apt to contain many dangling and wrong bonds, and accordingly bulk samples are preferred in the present study.
- [15] K. Tanaka, S. Nakayama, *Jpn. J. Appl. Phys.*, **38**, 3986 (1999).
- [16] R. A. Street, T. M. Searle, I. G. Austin, *Philos. Mag.*, **30**, 1181 (1974).
- [17] We put $d \approx 10 \mu\text{m}$ for bulk samples, which is the gap separation of the electrode.
- [18] Spectral data at low temperature can be obtained only at several wavelengths where intense monochromatic light is available, since the photoconduction dramatically reduces at low temperatures [1,3].
- [19] R. Zallen, R. E. Drews, R. L. Emerald, M. L. Slade, *Phys. Rev. Lett.*, **26**, 1564 (1971).
- [20] R. S. Sussmann, T. M. Searle, I. G. Austin, *Philos. Mag.*, **B44**, 665 (1981).
- [21] E. Tarnow, A. Antonelli, J. D. Joannopoulos, *Phys. Rev.*, **B34**, 4059 (1986).
- [22] K. Tanaka, *Appl. Phys. Lett.*, **73**, 3435 (1998).
- [23] K. Nagata, Y. Miyamoto, H. Nishimura, H. Suzuki, S. Yamasaki, *Jpn. J. Appl. Phys.*, **24**, L858 (1985).
- [24] N. S. Platakis, *J. Non-Cryst. Solids*, **24**, 365 (1977).
- [25] M. Saji, H. Kubo, *Nagoya Kougyou Daigaku Gakuhou*, **32**, 213 (1980).
- [26] D. E. Aspens, J. C. Philips, K. L. Tai, P. M. Bridenbaugh, *Phys. Rev.*, **B23**, 816 (1981).
- [27] H. Tichá, L. Tichý, E. Cernosková, *phys. stat. sol. (a)*, **119**, K135 (1983).
- [28] Note that the densities of a-Se and the ring-type crystals are comparable, which are less dense than that of the chain-type Se [23]. It is plausible that the similar densities govern the interaction between lone-pair electrons, which form the top of the valence band.
- [29] P. A. Fedders, D. A. Drabold, S. Nakhmanson, *Phys. Rev.*, **B58**, 15624 (1998).
- [30] G. Allan, C. Delerue, M. Lannoo, *Phys. Rev.*, **B57**, 6933 (1998).
- [31] Y. Watanabe, H. Kawazoe, M. Yamane, *J. Non-Cryst. Solids*, **95&96**, 365 (1987).
- [32] K. Weiser, M. H. Brodsky, *Phys. Rev.*, **B1**, 791 (1970).